

The Reactivity of *N*-Coordinated Amides in Metallopeptide Frameworks: Molecular Events in Metal-Induced Pathogenic Pathways?

Nicole Niklas,^[a] Frank Hampel,^[b] Günter Liehr,^[a] Achim Zahl,^[a] and Ralf Alsasser*^[a]

Abstract: The amino acid derived tertiary amide ligand *tert*-butoxycarbonyl-(*S*)-alanine-*N,N*-bis(picoyl)amide (Boc-(*S*)-Ala-bpa, **1**) has been synthesized as a model for metal-coordinating peptide frameworks. Its reactions with copper(II) and cadmium(II) salts have been studied. Binding of Cu²⁺ results in amide bond cleavage and formation of [(bpa)(solvent)Cu]²⁺ complexes. In contrast, the stable, eight-coordinate complex [(Boc-(*S*)-Ala-bpa)Cd(NO₃)₂] (**5**) has been isolated and characterized by X-ray crystallography. An unusual tertiary amide nitrogen coordination is observed in **5**; this gives rise to significantly reduced *cis*–*trans* isomerization barriers. Possible implications for metal-induced conformational changes in proteins are discussed.

Keywords: bioinorganic chemistry • cadmium • *cis*–*trans* isomerization • copper • solvolysis

Introduction

Metal complexes containing *N*-coordinated tertiary carboxamide ligands are rather exotic species, and it is easy to compile all the structures of this type listed in the Cambridge Database. The only classical Werner-type complex is (*N,N*-bispicolybenzoic acid amide)copper(II) dichloride, crystallized by Lectka et al.^[1] A few more examples have been characterized in organometallic compounds^[2–6] and with structurally related urea-derived ligands.^[7–12] Interestingly, it has been predicted that this coordination mode should lower the barrier to *cis*–*trans* isomerization about the C–N bond of amides in peptides.^[13] However, it has been taken as a rule that metal ions would never bind to the tertiary nitrogen atoms of peptidyl–prolyl bonds.^[14] This paradigm has recently been challenged; Lectka and co-workers have described the potential of metal ions to catalyze amide *cis*–*trans* isomerization in synthetic polyproline peptides.^[15] Crystallographic evidence for the involvement of a tertiary amide function involving metal–nitrogen coordination was obtained from

the model study cited above.^[1] In their publications, Lectka et al. have proposed the utilization of synthetic metal ion catalysts for peptide-folding reactions. This is an exciting possibility, since *cis*–*trans* isomerization about peptidyl–prolyl amide bonds has attracted much attention as the rate-limiting folding step in many proteins.^[16–19]

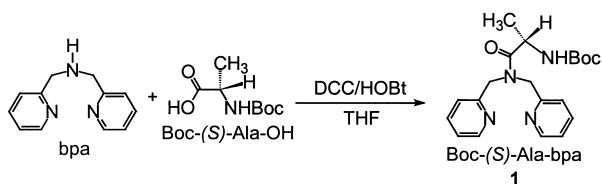
However, difficulties arise because the chemistry of *N*-coordinated tertiary amides is more complex than depicted above. In particular, C–N bond cleavage may provide a second major reaction pathway in addition to *cis*–*trans* isomerization. The copper-mediated hydrolysis of a tertiary amide bond in glycylsarcosyl-L-histidylglycine (Gly-Sar-His-Gly) has recently been reported by Ueda et al.^[20] In the early 1970s, Houghton and Puttner studied amide bond cleavage reactions in copper complexes of *N,N*-bispicolyloxycarbonyl amides.^[21] As mentioned above, Lectka et al. crystallized an analogue of the reactive intermediate and used it in their *cis*–*trans* isomerization studies.^[1]

The growing evidence for *N*-coordinated tertiary amides in synthetic metal peptide complexes suggests that this unusual binding mode may also occur in biological systems. If so, several questions arise concerning its consequences. This paper focuses on the different conditions that favor either *cis*–*trans* isomerization or bond cleavage. The effects of different metal ions, coordination geometries, ligand donor sets, chelate rings, and amino acid sequences are not yet understood at any detail. We have studied some of these aspects using the novel tertiary carboxamide ligand *tert*-butoxycarbonyl-L-alanine bispicolyamide (Boc-Ala-bpa, **1**), shown in Scheme 1. This compound belongs to a family of chelating amino acid derivatives which has been developed in

[a] Dr. R. Alsasser, Dipl.-Chem. N. Niklas, Akad. Oberrat Dr. G. Liehr, Dr. A. Zahl
Institute of Inorganic Chemistry, University of Erlangen
Egerlandstrasse 1, 91058 Erlangen (Germany)
Fax: (49) 9131-852-7387
E-mail: alsasser@chemie.uni-erlangen.de

[b] Akad. Rat Dr. F. Hampel
Institute of Organic Chemistry, University of Erlangen
Henkestrasse 42, 91054 Erlangen (Germany)

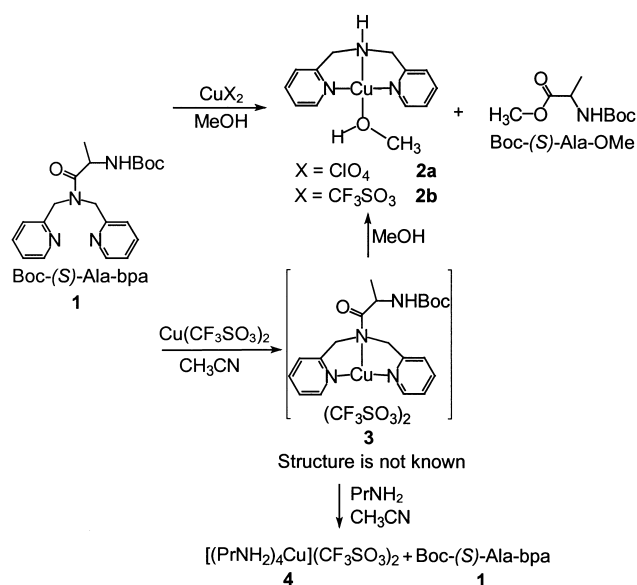
Supporting information for this article is available on the WWW under <http://www.wiley-vch.de/home/chemistry/> or from the author.

Scheme 1. Synthesis of the ligand Boc-(S)-Ala-bpa (**1**).

our research group.^[22, 23] Our ligands are designed to provide a well-defined metal binding site in combination with a weakly or noncoordinating, peptide-analogous periphery. These features facilitate the formation of weak interactions between metal ions and a biologically relevant environment. A particularly interesting and unusual example of such an interaction is the tertiary amide nitrogen coordination in copper(II) and cadmium(II) complexes of **1**. Both reactions, *cis-trans* isomerization and bond cleavage, are described below. The chiral urethane-protected (*S*)-alanine substituent is shown to play a role in the stereochemistry and reactivity of our complexes. Finally, in the conclusion, we propose a possible role of *N*-coordinated tertiary carboxamides in pathogenic reactions of metal ions.

Results

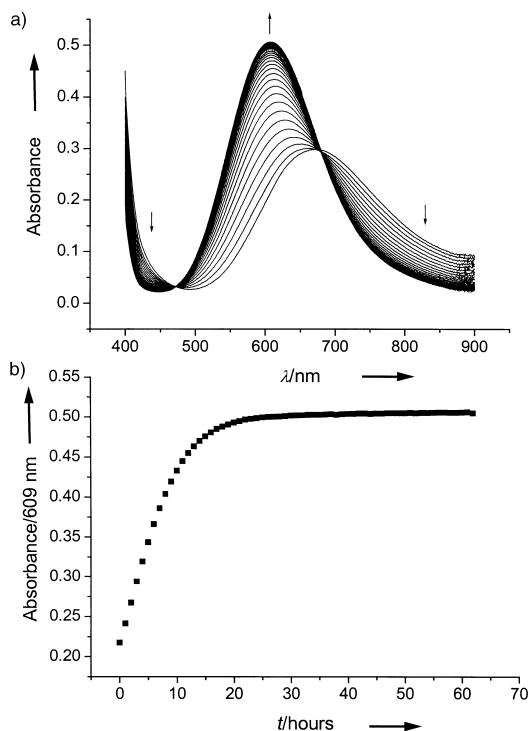
Synthesis: Scheme 1 shows the synthesis of Boc-(*S*)-Ala-bpa (**1**) from bispicolylamine (bpa) and *N*-*tert*-butoxycarbonyl-L-alanine. Its reactions with copper(II) salts are summarized in Scheme 2. In methanol, the alcoholysis products [(bpa)Cu]X₂

Scheme 2. Reactions of **1** with Cu(ClO₄)₂ and Cu(CF₃SO₃)₂.

(X = perchlorate, **2a**; X = triflate, **2b**) and Boc-Ala-OMe are obtained in high yields of over 80% after purification. The precursor complex [(Boc-Ala-bpa)Cu](OTf)₂ (**3**) can be obtained as a blue solid from anhydrous Cu(OTf)₂ and **1** in dry acetonitrile. By analogy with the structurally character-

ized complex [(bpa-C(O)Ph)CuCl₂]^[11] we propose the amide *N*-coordinated structure **3**.

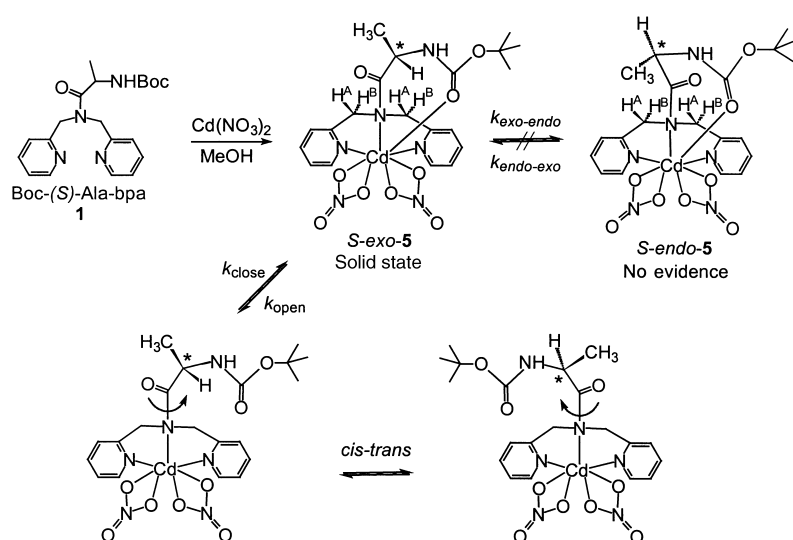
When treated with excess methanol, **3** undergoes quantitative alcoholysis, with formation of **2b**. This relatively slow reaction can be conveniently monitored by UV/Vis spectroscopy. Figure 1 shows representative plots of time-dependent

Figure 1. a) Spectra and b) kinetic trace at $\lambda = 609$ nm for the reaction of **3** with methanol in acetonitrile; [**3**] = 5×10^{-3} M, [MeOH] = 1.85 M.

spectra and the corresponding kinetic trace obtained by following the absorbance at 609 nm. A large 370-fold excess of methanol was applied in order to assure pseudo-first order measurement conditions. Under the measurement conditions the reaction was complete after approximately 24 hours. No simple kinetics were observed; attempts to fit the curve shown in Figure 1 by using one or two exponential functions failed. We think that the data may be obscured by slow ligand-exchange processes involving acetonitrile, methanol, the tertiary amide group, and the urethane function.

The facile substitution of [(bpa)Cu]²⁺ by methanol prompted us to treat **3** with an excess of *n*-propylamine in dry acetonitrile. This was done in order to evaluate whether our complex may be a useful reagent for amide-coupling reactions in peptide synthesis. However, we only observed decomplexation of copper(II), with formation of the free ligand **1** and a mixture of *n*-propylamine complexes. Elemental analysis data indicate an approximate stoichiometry of [(Pr-NH₂)₄Cu]²⁺ (**4**) for the latter.

In contrast to the solvolysis of **3**, a stable complex was obtained on treatment of ligand **1** with cadmium(II) nitrate in methanol. This is shown in Scheme 3, which describes the formation and structural mobility of [(Boc-Ala-bpa)Cd(NO₃)₂] (**5**). Two diastereomeric structures of **5** are possible, with the (*S*)-alanine methyl group oriented *endo* or *exo* with

Scheme 3. Synthesis and stereochemistry of $[(\text{Boc-(S)-Ala-bpa})\text{Cd}(\text{NO}_3)_2]$ (**5**).

respect to the 7-membered chelate ring. However, only the *exo* isomer is observed in the crystal structure. As explained later, this isomer is also dominant at low temperatures in solution, and no evidence has been observed for the *endo-exo* equilibrium shown in Scheme 3. Above approximately 0 °C, the chelate ring is open and *cis-trans* isomerization occurs.

Structures: X-ray structure analyses were obtained for the ligand **1**, the cleavage product **2a**, and the cadmium(II)

complex **5**. Crystallographic parameters are summarized in Table 1. We start with a discussion of the structure of **2a** in order to facilitate a direct comparison between the ligand geometries in **1** and **5**.

The distorted octahedral structure of bispicolyamine copper(II) diperchlorate (**2a**) is shown in Figure 2. A severe positional disorder refined well as two superimposed cations connected by a center of inversion. The metal center is located in the center of an idealized square plane formed by the three nitrogen donors of bpa and the oxygen atom of a methanol molecule. Two distant axial perchlorate ions complete the structure. To the

best of our knowledge, **2a** is the first structurally characterized example of a six-coordinate $[(\text{bpa})\text{Cu}]^{2+}$ complex with weakly coordinating anions and a 1:1 ligand to metal stoichiometry. The only related example in the literature is the recently reported trigonal-bipyramidal compound $[(\text{bpa})\text{Cu}(\text{NO}_3)_2]$.^[24] However, both complexes show a meridional arrangement of bpa, and the bond distances and angles are in excellent agreement. Slightly longer bonds but similar chelate angles are observed in the sterically more crowded 2:1 complexes.^[25]

Table 1. Details of crystal structure analyses.

Compound	1	2a	5
Formula	$\text{C}_{20}\text{H}_{26}\text{N}_4\text{O}_3$	$\text{C}_{13}\text{H}_{17}\text{Cl}_2\text{CuN}_3\text{O}_9$	$\text{C}_{21.5}\text{H}_{29}\text{CdCl}_3\text{N}_6\text{O}_9$
Formula weight	370.45	493.74	734.26
Temperature [K]	183(2)	173(2)	173(2)
Wavelength [Å]	0.70930	0.71073	0.71073
Crystal system	orthorhombic	triclinic	monoclinic
Space group	$P2_12_12_1$	$P1$	$P2_1$
<i>a</i> [Å]	9.316(2)	8.271(1)	9.369(1)
<i>b</i> [Å]	10.117(2)	8.592(1)	17.236(1)
<i>c</i> [Å]	20.976(2)	15.058 (1)	18.930(1)
α [°]	90	102.564(5)	90
β [°]	90	90.929(5)	91.392(1)
γ [°]	90	117.133(6)	90
Volume [Å ³]	1977.0(2)	921.3(1)	3056.0(1)
<i>Z</i>	4	2	4
Calculated density [Mg m ⁻³]	1.243	1.780	1.596
Absorption coefficient [mm ⁻¹]	0.09	1.53	1.03
<i>F</i> (000)	792	502	1484
Crystal size [mm ³]	0.80 × 0.43 × 0.23	0.30 × 0.20 × 0.20	0.40 × 0.40 × 0.30
θ -range [°]	2.80–21.90	1.40–26.05	1.60–25.06
Index ranges	$0 \leq h \leq 9$ $0 \leq k \leq 10$ $-21 \leq l \leq 22$	$-10 \leq h \leq 9$ $-10 \leq k \leq 10$ $-18 \leq l \leq 18$	$-11 \leq h \leq 11$ $-20 \leq k \leq 18$ $-22 \leq l \leq 22$
Reflects. collected/unique	2426/2426	5698/3502	9814/9814
Data/restr./parameters	2426/6/244	3502/6/288	9814/7/743
GOOF on <i>F</i> ²	0.884	1.100	1.077
Final <i>R</i> indices	$R1 = 0.0283$ [$I > 2\sigma(I)$] $wR2 = 0.0820$	$R1 = 0.0626$ [$I > 2\sigma(I)$] $wR2 = 0.1226$	$R1 = 0.0427$ [$I > 2\sigma(I)$] $wR2 = 0.1201$
<i>R</i> indices (all data)	$R1 = 0.0324$ $wR2 = 0.0957$	$R1 = 0.0936$ $wR2 = 0.1338$	$R1 = 0.0463$ $wR2 = 0.1238$
Largest diff. peak and hole [$e \text{ \AA}^{-3}$]	0.140 and –0.170	0.519 and –0.377	1.249 and –0.827

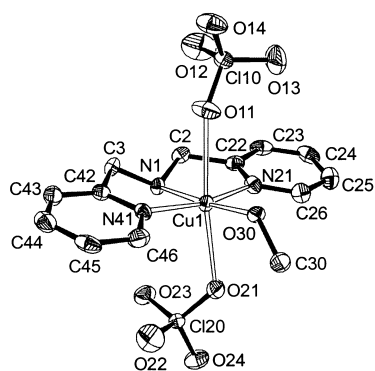


Figure 2. Ortep plot of **2a** (30% ellipsoids). Selected bond lengths [Å] and angles [°] (standard deviations in parentheses): Cu1–N1 = 2.001(5), Cu1–N21 = 1.973(4), Cu1–N41 = 1.971(4), Cu1–O30 = 1.986(4), Cu1–O11 = 2.556(7), Cu1–O21 = 2.432, N21–Cu1–N1 = 82.8(2), N41–Cu1–N1 = 82.7(2), N21–Cu1–N41 = 164.6(2), N21–Cu1–O30 = 98.0(2), N41–Cu1–O30 = 95.8(2), N1–Cu1–O30 = 174.1(2).

The structure of Boc-Ala-bpa (**1**) is shown in Figure 3. Most interesting for the following discussion are the geometries of the tertiary amide and urethane functional groups. Both moieties are almost planar, with C–N–C–O torsion angles of

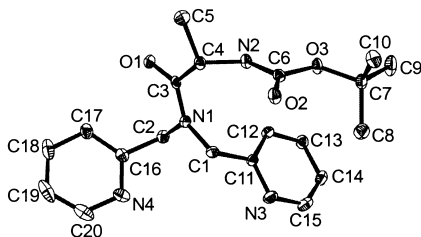


Figure 3. Ortep plot of **1** (30% ellipsoids). Selected bond lengths [Å], angles [°], and torsion angles [°] (standard deviations in parentheses): O1–C3 = 1.226(7), N1–C3 = 1.353(8), N2–C6 = 1.333(8), O3–C6 = 1.37(8), O2–C6 = 1.227(7), O1–C3–C4 = 120.2(2), C1–N1–C2 = 115.6(2), C4–N2–C6 = 123.5(2), C1–N1–C3–O1 = –172.2(2), C2–N1–C3–C4 = 180.0(2), C4–N2–C6–O3 = –174.57(2).

172° and 175°, respectively. The bond lengths C3–N1 (1.35 Å), C3–O1 (1.23 Å), C6–N2 (1.33 Å), and C6–O2 (1.23 Å) are as expected for amide groups in a peptide chain.^[26] A hitherto unknown chelating amide-*N*-, amide-*O*-binding mode of this dipeptide-analogous framework is observed in the structure of **5**, which is shown in Figure 4.

Two independent complexes **5** are present in the unit cell. They are distinguished by an asymmetric distribution of three co-crystallized dichloromethane solvent molecules. This results in slightly different bond lengths and angles, which are most probably due to packing effects. Both sets of bond lengths and angles are given in the legend of Figure 4. In the following section we will use the data for Cd1 rather than Cd1', but will discuss the differences when a comparison is appropriate.

The first coordination sphere of **5** is best described as a triply capped distorted square pyramid. Its base is formed by the two pyridine nitrogen donors and two oxygen atoms, provided by the urethane carbonyl group and one nitrate anion. These are the four nearest donors to Cd1, at an average distance of 2.31 Å. A slightly longer bond of 2.41 Å to the

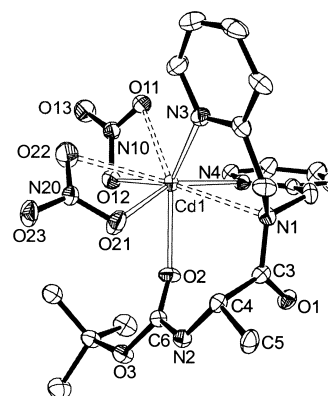


Figure 4. Ortep plot of **5** (30% ellipsoids). Selected bond lengths [Å], angles [°], and torsion angles [°] (standard deviations in parentheses); values are listed for both independent molecules in the unit cell: Cd1–N1 = 2.755(5), Cd1–N3 = 2.316(5), Cd1–N4 = 2.299(4), Cd1–O2 = 2.343(4), Cd1–O11 = 2.503(4), Cd1–O12 = 2.414(5), Cd1–O21 = 2.299(4), Cd1–O22 = 2.751(6), O1–C3 = 1.209(7), N1–C3 = 1.417(8), N2–C6 = 1.342(7), O3–C6 = 1.337(7), O2–C6 = 1.234(6), C1–N1–C2 = 112.8(5), C1–N1–C3–O1 = –144.6(6), C2–N1–C3–C4 = –175.7(5), Cd1'–N1' = 2.771(5), Cd1'–N3' = 2.345(5), Cd1'–N4' = 2.331(6), Cd1'–O2' = 2.387(4), Cd1'–O11' = 2.415(5), Cd1'–O12' = 2.544(5), Cd1'–O21' = 2.355(6), Cd1'–O22' = 2.663(6), O1'–C3' = 1.228(7), N1'–C3' = 1.376(8), N2'–C6' = 1.335(8), O3'–C6' = 1.341(7), O2'–C6' = 1.234(7), C1'–N1'–C2' = 114.1(5), C1'–N1'–C3'–O1' = –150.3(6), C2'–N1'–C3'–C4' = –177.0(5).

nitrate oxygen atom O12 in the apical position is observed. Two neighboring triangular faces are capped by the remaining nitrate oxygen atoms. The Cd–O bond distances are relatively long at 2.75 and 2.50 Å. Finally, the tertiary amide nitrogen atom N1 is located above the basal plane, 2.76 Å away from Cd1.

Most interesting in the structure of **5** is its peptide-analogous diamide part. As mentioned above, the urethane group shows the normal carbonyl oxygen binding that has been described for several cadmium complexes with peptides^[27–29] and other carboxamide ligands.^[30, 31] This coordination mode does not significantly affect the geometry of the bound amide. The bond lengths and torsion angles remain almost unchanged. This is in marked contrast to the *N*-coordinated tertiary amide function. Though the cadmium–nitrogen bond is relatively weak, it results in a significant deplanarization at N1. This is clearly seen in Figure 5, which shows a comparison of the tertiary amide

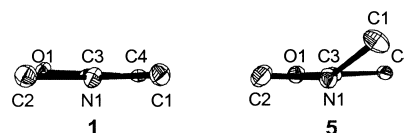


Figure 5. Comparison of the tertiary amide structures in **1** and in **5**.

functions in **1** and in **5**. The C1–N1–C3–O1 torsion angle is significantly reduced from –172° in the ligand to –144° in the complex. For the second complex in the unit cell a value of 150° is observed. Small changes appear in the C3–N1 and C3–O1 bond lengths, but these are negligible for C3'–N1' and C3'–O1' and so may not be significant.

NMR Studies: In order to evaluate the barriers to *cis*–*trans* isomerization reactions for **1** and **5**, we studied their temperature-dependent ^1H NMR spectra. The pyridine and methylene parts of the spectra at three different temperatures are compared in Figure 6. For **1** in CDBr_3 at 25°C , two clearly separated sets of signals are observed for each of the pyridine protons pyH6 (Figure 6a: A) and pyH4 (B). Three sets of signals (F) are observed for the diastereotopic py- CH_2 protons. Coalescence is observed only at temperatures above 80°C .

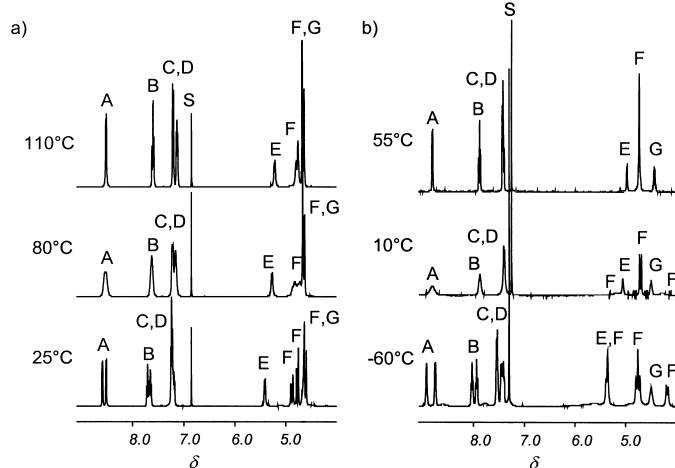


Figure 6. Temperature-dependent ^1H NMR spectra (400 MHz) of: a) **1** in CDBr_3 , and b) **5** in CDCl_3 . Signals are labeled as follows. A: py-H6, B: py-H4, C: py-H5, D: py-H3, E: Boc-NH, F: py- CH_2 , G: $^{\alpha}\text{CH}$, S: solvent.

In contrast, the two picolyl substituents in the cadmium complex **5** are indistinguishable at room temperature. Fully resolved spectra of **5** in CDCl_3 are only obtained at temperatures below -50°C (Figure 6b). Coalescence is observed at approximately 0°C for the pyridine signals A and B, and slightly above room temperature for the methylene resonances F. The pyridine resonance pattern A–D of **5** at -60°C is similar to that of **1** at $+25^\circ\text{C}$, except for a characteristic low-field shift of the signals A and B. Interestingly, no evidence is observed for the existence of the two different diastereoisomers shown in Scheme 3. At temperatures between 0°C and -40°C a significant broadening of the lowest field pyH6 resonance signal is observed. The other signal of set A is not affected. Interesting are the methylene signals (F) of **5**, which are split into three sets with very large chemical shift differences. The central multiplet appears at $\delta = 4.8$, which is close to the values observed for **1**. We therefore assign this signal to the protons H^{B} in Scheme 3, which are oriented away from the metal ion. Of the two signals for protons H^{A} , one appears at higher field ($\delta = 4.2$) and one at lower ($\delta = 5.2$) field. From these data we are not able to assign these resonances to a particular ring.

Rate constants were obtained by simulating the pyridine regions of the spectra with the program WIN-Dynamics.^[32] Activation parameters were determined from the linear Eyring plots shown in Figure 7. For ligand **1** (Figure 7a) the activation enthalpy ΔH^\ddagger is $17.6 \pm 0.9 \text{ kcal mol}^{-1}$ and the activation entropy ΔS^\ddagger is $-1.1 \pm 2.7 \text{ cal K}^{-1} \text{ mol}^{-1}$. Only data obtained above 50°C were used, because the rates at lower

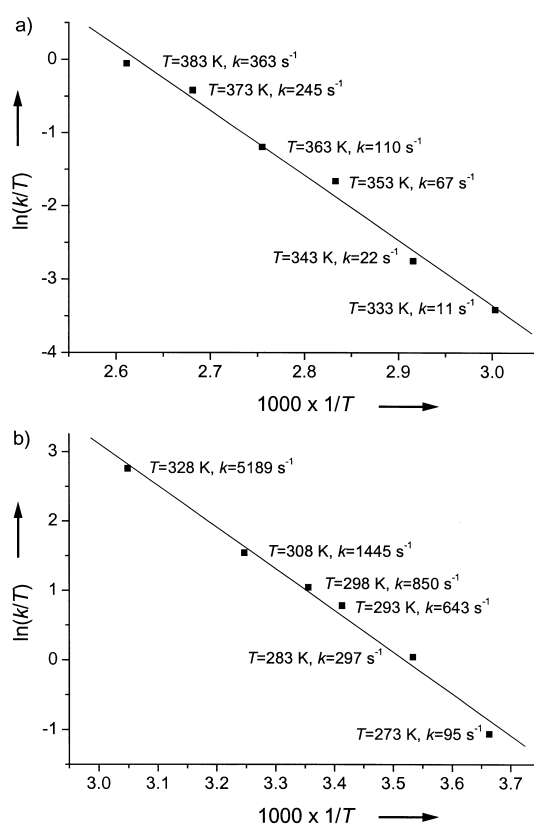


Figure 7. Eyring plots ($\ln(kT^{-1})$ vs. T^{-1}) of the kinetic data obtained by fitting the temperature-dependent ^1H NMR spectra (400 MHz) of a) **1** and b) **5**. Temperatures and observed rate constants are listed for each data point.

temperatures were too small to be determined. In the case of **5** (Figure 7b), data collected at temperatures above 0°C were interpreted. Activation parameters $\Delta H^\ddagger = 11.9 \pm 0.7 \text{ kcal mol}^{-1}$ and $\Delta S^\ddagger = -5.3 \pm 2.1 \text{ cal K}^{-1} \text{ mol}^{-1}$ are derived. A reliable simulation of the spectra at lower temperatures was not possible.

Discussion

The ligand Boc-Ala-bpa (**1**) was designed to serve as a model for metal-binding peptides and proteins. It has two amide groups that closely resemble a polypeptide backbone and two pyridine donors that mimic metal-coordinating side chains, such as the imidazole ring in histidine. All four functional groups of **1** may participate in metal ion binding, as is demonstrated by the structure of its cadmium(II) complex (**5**).

Our ligand design is well suited to study the effects of noncoordinating amino acid side chains on the coordination properties and reactivity of our compounds. This is nicely demonstrated by the stereochemistry of **5**. Of the two different diastereoisomers shown in Scheme 3, only the *exo* isomer is present in the solid state. This orientation must also be energetically favored in solution, since only one isomer is seen in the NMR spectra below -40°C . Greater stability of one isomer would require different rate constants $k(\textit{exo} \rightarrow \textit{endo})$ and $k(\textit{endo} \rightarrow \textit{exo})$ if *cis*–*trans* isomerization were to occur in the *tert*-butoxycarbonyl-coordinated complex shown

in the upper part of Scheme 3. A nonlinear Eyring plot would be expected. However, this is not the case if spectra obtained at elevated temperatures are interpreted. An alternative mechanism is provided by the chelate ring-opening shown in the lower part of Scheme 3. In the reactive isomer, the ligand **1** is only tridentate and the amino acid substituent is flexible. Steric constraints are not effective in this conformation and the forward and back reactions of the *cis*–*trans* isomerization equilibrium are expected to occur with similar rates. The pre-equilibrium $k_{\text{open}}/k_{\text{close}}$ may also explain 1) the asymmetric broadening of one pyH6 resonance signal below 0 °C and 2) the difficulty in simulating spectra at lower temperatures. Furthermore, our activation parameters are in excellent agreement with values reported for copper complexes of the tridentate ligand *N,N*-bispicolyl benzoic acid amide. The latter data were obtained by Lectka and co-workers^[1] from saturation transfer measurements. It is interesting that Cd²⁺ and Cu²⁺ have similar effects on *cis*–*trans* isomerization rates while giving rise to completely different reactivities in methanol.

At 25 °C, the free activation enthalpies ΔG^\ddagger of *cis*–*trans* isomerization are 17.8 kcal mol⁻¹ for **1** and 13.4 kcal mol⁻¹ for **5**. When compared with literature data for other activated amide isomerization reactions, such as nucleophilic^[33] or intramolecular^[34] catalysis, a $\Delta\Delta G^\ddagger$ value of –4.4 kcal mol⁻¹ indicates a very efficient lowering of the activation barrier. The rate enhancement at room temperature is approximately 1000-fold. This means a tremendous conformational labilization through the relatively weak Cd–N1 interaction. On the other hand, our results suggest that a rigid chelate geometry may suppress the *cis*–*trans* isomerization reactivity of *N*-coordinated amides.

The question remains of what reactivity would be expected from an *N*-coordinated tertiary amide complex in a biological peptide: *cis*–*trans* isomerization or bond breakage? Lectka et al. have demonstrated that copper(II) ions catalyze the *cis*–*trans* isomerization of peptide bonds.^[1, 15] We observe the efficient methanolysis of the C–N bond upon coordination of the strong Lewis acid Cu²⁺. This result agrees with observations by the groups of Houghton,^[21] Sayre,^[35] and Ueda.^[20] However, while copper-induced bond cleavage proceeds with high yields, it is also very slow. In addition, *N*-coordinated tertiary amides are poor ligands. This is evident from our decomplexation reaction with *n*-propylamine. For their NMR studies, Lectka et al. have always used catalytic amounts of copper(II) ions. Catalysis implies that the metal ion is mobile and rapidly equilibrates between different binding sites. Thus, transient binding of Cu²⁺ to a tertiary amide nitrogen atom is sufficient to induce the fast *cis*–*trans* isomerization process, but it would almost certainly not cause bond cleavage. It is interesting to note that Cd²⁺ has recently been shown to facilitate amide bond alcoholysis when it is carbonyl-*O* coordinated.^[36] In our *N*-coordinated complex we have not observed any evidence for this reaction.

Conclusion

In this study we have introduced a model system for tertiary amide complexes in biologically relevant systems. Character-

istic for our compounds is their structural mobility. In the case of cadmium(II), this reveals itself in the urethane coordination–decoordination equilibrium that occurs prior to *cis*–*trans* isomerization. Even more dramatic is the demetalation of [(Boc-Ala-bpa)Cu](OTf)₂ (**3**) by *n*-propylamine. Their low complex stabilities are probably the reason why *N*-coordinated peptidyl–prolyl functions have not yet been observed in biological systems. This is an important consideration for the expected reactivity of such species.

Both relevant reaction pathways, bond breakage and *cis*–*trans* isomerization, occur in our complexes. While the former is slow, the latter requires only a few milliseconds at room temperature. We therefore conclude that bond cleavage upon tertiary amide coordination is a highly unlikely event in proteins. However, transient binding of a metal ion would be sufficient to induce *cis*–*trans* isomerization reactions. As a consequence, conformational changes in peptides and proteins would be expected. Such processes have been widely discussed in connection with deleterious effects of metal ions. Examples are the pathogenic interactions of cadmium(II) ions with transcription factors^[37] or DNA repair proteins,^[38] as well as the formation of abnormal prion protein isoforms, which are the infectious agents in neurodegenerative diseases.^[39–42] Not much is known about the molecular origin of pathogenic structural variations in proteins. At least in some cases, metal-induced *cis*–*trans* isomerization reactions may provide a reasonable and experimentally verifiable explanation. We think that this hypothesis should be considered as a starting point for detailed spectroscopic and mechanistic studies. Intriguingly, a proline residue is present in the copper binding site of prion proteins.^[43–46]

Experimental Section

General methods: Spectra and analytical data were recorded with the following instruments: ¹H and ¹³C NMR: room temperature spectra—Bruker Avance DPX300, temperature-dependent spectra—Bruker Avance DRX400WB. All chemical shifts are referenced to TMS as internal standard with high-frequency shifts recorded as positive. IR: Mattson Polaris FT-IR. Elemental analysis: Carlo Erba EA 1106. UV/Vis: Varian Cary 1G Spectrophotometer. EPR: Bruker ESP 300E. All spectra were recorded at 120 K in frozen methanol or acetonitrile.

Unless noted otherwise, all reactions were carried out under an atmosphere of dry nitrogen. Anhydrous solvents were purchased from Fluka and stored under nitrogen. Solvents were used without further purification. All other reagents were of commercially available reagent-grade quality. Boc-L-Ala-OH was obtained from Bachem and CDBr₃ from Acros Organics. All other chemicals were purchased from Aldrich. Bis(picolyl)amine (bpa) was synthesized according to published procedures.^[47, 48]

Boc-Ala-bpa (1): A solution of Boc-L-Ala-OH (5.00 g, 26.40 mmol), bispicolylamine (5.25 g, 26.40 mmol), and 1-hydroxybenzotriazole (HOBt) (4.28 g, 31.70 mmol) in THF (50 mL) was cooled to –10 °C in an ice/salt bath. *N,N'*-Dicyclohexylcarbodiimide (DCC) (6.54 g, 31.70 mmol) was dissolved in a small volume of THF and added in one portion to the solution. The mixture was stirred at –10 °C over a period of 1 h and then allowed to warm up to room temperature. Stirring was continued overnight. The suspension was filtered off and washed twice with small amounts of cold (4 °C) THF. The filtrate was concentrated to dryness. The residue was treated with CH₂Cl₂ (50 mL) and washed three times with 0.05 M citric acid (50 mL), once with water (50 mL), three times with NaHCO₃ solution (0.5 M, 50 mL), and once with water (50 mL). The organic phase was dried over MgSO₄, filtered, and reduced by approximately half. After storage at

–20 °C overnight, the mixture was filtered to remove excess dicyclohexylurea. Addition of Et₂O to the clear CH₂Cl₂ filtrate and storage at –20 °C afforded the product as a colorless, microcrystalline solid. Suitable crystals for an X-ray structure analysis were obtained by recrystallization of the product from CH₂Cl₂/Et₂O at 4 °C. Yield: 5.12 g (13.8 mmol, 52 %); ¹H NMR (300 MHz, CDCl₃), δ = 1.34 (d, 3H; CH₃), 1.43 (s, 9H; C(CH₃)₃), 4.68 (d, ³J(H,H) = 17.2 Hz, 1H; py-CH^AH^B), 4.70 (d, ³J(H,H) = 15.4 Hz, 1H; py-CH^AH^B), 4.78 (m, 1H; ^aCH), 4.84 (d, ³J(H,H) = 15.5 Hz, 1H; py-CH^AH^B), 4.96 (d, ³J(H,H) = 17.2 Hz, 1H; py-CH^AH^B), 5.59 (d, ³J(H,H) = 7.3 Hz, 1H; NH), 7.20 (m, 4H; H₃-py, H₃'-py, H₅-py, H₅'-py), 7.63 (m, 2H; H₄-py, H₄'-py), 8.49, 8.55 (2 × d, ³J(H,H) = 4.8 Hz, ³J(H',H') = 4.6 Hz, 2H; H₆-py, H₆'-py); IR (KBr): $\tilde{\nu}$ = 1674 (CO urethane), 1660 (CO amide), 1591 (C=N); FD-MS (CDCl₃): *m/z*: 742 [2M + 2H]⁺, 370 [M]⁺; elemental analysis calcd (%) for C₂₀H₂₆N₄O₃ (370.5): C 64.85, H 7.07, N 15.12; found C 64.89, H 7.70, N 14.93.

Amide Cleavage Reactions: The following two reactions were carried out under air in p.a. grade solvents.

[(bpa)(H₂O)Cu](ClO₄)₂ (2a): Solid Cu(ClO₄)₂·6H₂O (441 mg, 1.19 mmol) was added in one portion to a stirred solution of Boc-Ala-bpa (441 mg, 1.19 mmol) in MeOH (10 mL). After several hours, a blue solid precipitated. Stirring was continued overnight at room temperature. The resulting suspension was stored in a refrigerator (–20 °C) in order to complete precipitation. The product was filtered off and dried in a vacuum. The C,H,N elemental analysis of this product is consistent with the formulation [(bpa)(H₂O)Cu](ClO₄)₂. Reported yields are for this product. Recrystallization from MeOH by slow evaporation of the solvent afforded blue needles suitable for X-ray structure analysis. The C,H,N elemental analysis of the crystals is consistent with the formulation [(bpa)(MeOH)Cu](ClO₄)₂. Both results are given below. Yield: 485 mg (1.01 mmol, 85 %); EPR (MeOH, 120 K): *g*_x = 2.02, *g*_y = 2.07, *g*_z = 2.26, *A*_z = 186 × 10^{–4} cm^{–1}; (MeCN, 120 K): *g* = 2.08 (isotropic spectrum); IR (KBr): $\tilde{\nu}$ = 1609 (C=N), 1143 (ClO₄), 1113 (ClO₄), 1090 (ClO₄); UV/Vis (MeOH): λ_{max} (lg ϵ) = 660 nm (1.95); (MeCN): λ_{max} (lg ϵ) = 605 nm (2.11); FAB-MS (nitrobenzyl alcohol): *m/z*: 262 [(bpa)Cu]⁺; elemental analysis calcd (%) for C₁₂Cl₂CuH₁₅N₃O₉ (479.7), [(bpa)(H₂O)Cu](ClO₄)₂, bulk sample: C 30.05, H 3.15, N 8.76; found C 30.27, H 3.18, N 8.54; elemental analysis calcd (%) for C₁₃Cl₂CuH₁₇N₃O₉ (493.7), [(bpa)(MeOH)Cu](ClO₄)₂, crystals: C 31.62, H 3.47, N 8.51; found C 31.56, H 3.59, N 8.81.

[(bpa)(H₂O)Cu](OTf)₂ (2b): Boc-Ala-bpa (303 mg, 0.82 mmol) was dissolved in MeOH (10 mL). After addition of Cu(OTf)₂ (296 mg, 0.82 mmol), the mixture was stirred overnight at RT. The solvent was removed in vacuo, and the crude product was treated with CH₂Cl₂ (5 mL). The resulting suspension was filtered and the blue residue dried in vacuo. Yield: 495 mg (0.68 mmol, 83 %); EPR (MeOH, 120 K): *g*_x = 2.01, *g*_y = 2.06, *g*_z = 2.26, *A*_z = 187 × 10^{–4} cm^{–1}; EPR (MeCN, 120 K): *g* = 2.07 (isotropic spectrum); IR (KBr): $\tilde{\nu}$ = 1614 (C=N), 1283 (OTf), 1246 (OTf), 1170 (OTf); UV/Vis (MeOH): λ_{max} (lg ϵ) = 661 nm (1.95); UV/Vis (CH₃CN): λ_{max} (lg ϵ) = 605 nm (2.10); FAB-MS (nitrobenzyl alcohol): *m/z*: 262 [(bpa)Cu]⁺, 411 [(bpa)Cu(OTf)]⁺; elemental analysis calcd (%) for C₁₄CuF₆H₁₅N₃O₇S₂ (579.0): C 29.05, H 2.61, N 7.26; found C 29.09, H 2.54, N 7.11.

Copper(II) and cadmium(II) complexes of Boc-Ala-bpa:

[(Boc-Ala-bpa)Cu](OTf)₂ (3): Solid Cu(OTf)₂ (181 mg, 0.50 mmol) was added in one portion to a stirred solution of Boc-Ala-bpa (185 mg, 0.50 mmol) in MeCN (10 mL). Stirring was continued overnight at room temperature, and the solvent was removed under vacuum. The crude product was dissolved in CH₂Cl₂ (10 mL). Diethyl ether was allowed to diffuse into this solution slowly at RT, until a blue oil separated. The supernatant was decanted and the residue dried in vacuo. Yield: 258 mg (0.35 mmol, 70 %); EPR (MeCN, 120 K): *g*_{||} = 2.31, *A*_{||} = 179 × 10^{–4} cm^{–1}, *g*_⊥ = 2.08; IR (KBr): $\tilde{\nu}$ = 1693 (br, CO amide + CO urethane), 1613 (C=N), 1261 (OTf), 1165 (OTf); UV/Vis (MeCN): λ_{max} (lg ϵ) = 672 nm (1.85). FAB-MS (nitrobenzyl alcohol): *m/z*: 433 [(Boc-Ala-bpa)Cu]⁺, 582 [(Boc-Ala-bpa)Cu(OTf)]⁺; elemental analysis calcd (%) for C₂₂CuF₆H₂₆N₄O₈S₂ (732.13): C 36.09, H 3.58, N 7.51, S 8.76; found C 36.21, H 3.89, N 7.79 S 8.37.

[(Boc-Ala-bpa)Cd(NO₃)₂] (5): Boc-Ala-bpa (500 mg, 1.35 mmol) was dissolved in MeOH (10 mL). Cd(NO₃)₂·4H₂O (417 mg, 1.35 mmol) was added, and the solution was stirred overnight at room temperature. After removal of solvent in vacuo, the residual solid was treated with CH₂Cl₂ (10 mL). The mixture was cooled to –20 °C and filtered. The filtrate was

reduced to approximately half of its volume, and Et₂O was added. Storage at –20 °C and repeated addition of Et₂O afforded the product as a white precipitate. The product was collected on a sintered-glass filter, dried in vacuo, and characterized by C,H,N elemental analysis, FAB-MS, and ¹H NMR. The assignment of ¹H NMR signals was assisted by ¹H,¹H-COSY spectra. Crystals suitable for X-ray structure analysis were obtained by recrystallization of the pure product from CH₂Cl₂/Et₂O at 4 °C. Yield: 637 mg (1.05 mmol, 78 %); ¹H NMR (300 MHz, CDCl₃), δ = 1.28 (d, 3H; CH₃), 1.32 (s, 9H; C(CH₃)₃), 1.67 (s, 2H; H₂O), ≈ 3.8–5.6 (br, 2H; py-CH^AH^B + py-CH^AH^B), 4.46 (m, 1H; ^aCH), 4.72 (d, ³J(H,H) = 15.5 Hz, 2H; py-CH^AH^B + py-CH^AH^B), 4.04 (d, ³J(H,H) = 4.5 Hz, 1H; NH), 7.43 (m, 4H; H₃-py, H₃'-py, H₅-py, H₅'-py), 7.90 (m, 2H; H₄-py, H₄'-py), 8.75 (br m, 2H; H₆-py, H₆'-py); IR (KBr): $\tilde{\nu}$ = 1703 (CO amide), 1665 (CO urethane), 1608 (C=N), 1440 (NO₃), 1383 (NO₃), 1298 (NO₃). FAB-MS (nitrobenzyl alcohol): *m/z*: 546 [(Boc-Ala-bpa)Cd(NO₃)₂]⁺, 490 [(Boc-Ala-bpa)-Cd(NO₃) – CH₂=C(CH₃)₂]⁺, 371 [Boc-Ala-bpa]⁺; elemental analysis calcd (%) for C₂₀CdH₂₆N₄O₈ (606.9): C 39.58, H 4.32, N 13.85; found C 39.82, H 4.54, N 13.79.

Treatment of [(Boc-Ala-bpa)Cu](OTf)₂ (2) with *n*-propylamine: A solution of Boc-Ala-bpa (574 mg, 1.55 mmol) and Cu(OTf)₂ (560 mg, 1.55 mmol) in MeCN (10 mL) was stirred for 1 h to generate **2**, which was not isolated. *n*-Propylamine (183.2 mg, 3.1 mmol) was added, and stirring was continued overnight. After removal of all solvent under vacuum, the residual solid was treated with CH₂Cl₂ (10 mL). A blue solid precipitated immediately, which was filtered and dried in vacuo. The IR spectrum exhibited no signals for the ligand Boc-Ala-bpa. C,H,N analytical data are best matched by the formulation [(NH₂CH₂CH₂CH₃)₄Cu](OTf)₂. FAB-MS of the filtrate showed a peak for the starting material [(Boc-Ala-bpa)Cu]⁺ at *m/z* = 433. The free ligand **1** was identified by the signal of [Boc-Ala-bpa]⁺ at *m/z* = 371 in the FD-MS. Pure Boc-Ala-bpa was isolated and characterized by ¹H NMR after flash column chromatography with methanol as the eluent. Yield: 400 mg (0.67 mmol); elemental analysis calcd (%) for C₁₄CuF₆H₃₆N₄O₆S₂ (598.1): C 28.11, H 6.07, N 9.37; found C 28.77, H 5.81, N 9.02.

X-ray data collection and structure refinement details: Crystal data and experimental conditions for **1**, **2a**, and **5** are listed in Table 1. The molecular structures are illustrated in Figures 3, 4, and 5. Selected bond lengths and angles, with standard deviations in parentheses, are presented in the respective Figure legends. Intensity data were collected with graphite monochromated Mo-*K*_α radiation on a Nonius CADMACH3 diffractometer (**1**) and on a Nonius KappaCCD area detector (**2a** and **5**). The collected reflections were corrected for Lorentz, polarization, and absorption^[49] effects. All structures were solved by direct methods and refined by full-matrix least-squares methods on *F*².^[50–52] Hydrogen atoms were calculated for idealized geometries and allowed to ride on their preceding atoms with isotropic displacement parameters tied to those of the adjacent atoms by a factor of 1.5.

Details of the crystal structure determinations have been deposited at the Cambridge Crystallographic Data Centre as supplementary publications no. CCDC 157427 (**1**), CCDC 157410 (**2a**), and CCDC 157411 (**5**). Copies of the data can be obtained free of charge on application to the CCDC, 12 Union Road, Cambridge CB2 1EZ (UK) [Fax: (+44) 1223-336033; E-mail: deposit@ccdc.cam.ac.uk].

Simulation of temperature-dependent ¹H NMR spectra: The program WIN-Dynamics was used for all calculations.^[32] Starting values for chemical-shift values and coupling constants were obtained from spectra at low temperatures. Starting values for rate constants were estimated from the coalescence temperatures^[53] or obtained by guessing and comparison of simulated and experimental curves. In a first iteration cycle the chemical shift values were refined to convergence. This was followed by refinement of the rate constants. Plots of simulated and experimental spectra are available as supporting information.

Acknowledgement

The authors gratefully acknowledge financial support from the Deutsche Forschungsgemeinschaft and from the Bayerischer Prion-Forschungsverbund. We thank Prof. Rudi van Eldik for his generous support.

- [1] C. Cox, D. Ferraris, N. N. Murthy, T. Lectka, *J. Am. Chem. Soc.* **1996**, *118*, 5332.
- [2] J.-C. Wang, C.-H. Sun, T. J. Chow, L.-K. Liu, *Acta Cryst. Sect. C* **1991**, *47*, 2459.
- [3] F. Müller, G. van Koten, K. Vrieze, B. Krijnan, C. H. Stam, *J. Chem. Soc. Chem. Commun.* **1986**, 150.
- [4] F. Müller, G. van Koten, M. J. A. Kraakman, K. Vrieze, D. Heijdenrijk, M. C. Zoutberg, *Organomet.* **1989**, *8*, 1331.
- [5] F. Müller, G. van Koten, K. Vrieze, D. Heijdenrijk, *Organomet.* **1989**, *8*, 33.
- [6] L. H. Polm, G. van Koten, K. Vrieze, C. H. Stam, W. C. J. van Tunen, *J. Chem. Soc. Chem. Commun.* **1983**, 1177.
- [7] D. Wester, G. J. Palenik, *J. Am. Chem. Soc.* **1974**, *96*, 7565.
- [8] P. S. Gentile, J. White, S. Haddad, *Inorg. Chim. Acta* **1974**, *8*, 97.
- [9] P. Maslak, J. J. Szepanski, M. Parvez, *J. Am. Chem. Soc.* **1991**, *113*, 1062.
- [10] D. P. Fairlie, T. C. Woon, W. A. Wickramasinghe, A. C. Willis, *Inorg. Chem.* **1994**, *33*, 6425.
- [11] H. Rauter, E. C. Hillgeris, A. Erxleben, B. Lippert, *J. Am. Chem. Soc.* **1994**, *116*, 616.
- [12] E. Colacio, R. Cuesta, J. M. Gutierrez-Zorrilla, A. Luque, P. Roman, T. Giraldi, M. R. Taylor, *Inorg. Chem.* **1996**, 4232.
- [13] H. Sigel, R. B. Martin, *Chem. Rev.* **1982**, *82*, 385.
- [14] L. D. Pettit, I. Steel, G. Formicka-Kozłowska, T. Tatarowski, M. Bataille, *J. Chem. Soc. Dalton Trans.* **1985**, 535.
- [15] C. Cox, T. Lectka, *Acc. Chem. Res.* **2000**, *33*, 849.
- [16] F. X. Schmid in *Protein Folding* (Ed.: T. E. Creighton), Freeman, New York, **1992**, p. 197.
- [17] W. A. Houry, H. A. Scheraga, *Biochemistry* **1996**, *35*, 11 719.
- [18] L. Ma, L. C. Hsieh-Wilson, P. G. Schultz, *Proc. Natl. Acad. Sci. USA* **1998**, *95*, 7251.
- [19] G. Scherer, M. L. Kramer, M. Schutkowski, U. Reimer, G. Fischer, *J. Am. Chem. Soc.* **1998**, *120*, 5568.
- [20] J. Ueda, M. Miyazaki, Y. Matsushima, A. Hanaki, *J. Inorg. Biochem.* **1996**, *63*, 29.
- [21] R. P. Houghton, R. R. Puttner, *Chem. Commun.* **1970**, 1270.
- [22] N. Niklas, O. Walter, R. Alsfasser, *Eur. J. Inorg. Chem.* **2000**, 1723.
- [23] N. Niklas, S. Wolf, G. Liehr, C. E. Anson, A. K. Powell, R. Alsfasser, *Inorg. Chim. Acta* **2001**, *314*, 126.
- [24] M. Palaniandavar, S. Mahadevan, M. Köckerling, G. Henkel, *J. Chem. Soc. Dalton Trans.* **2000**, 1151.
- [25] M. Palaniandavar, R. J. Butcher, A. W. Addison, *Inorg. Chem.* **1996**, *35*, 467.
- [26] H. D. Jakubke, *Peptide*, Spektrum Akademischer, Heidelberg, **1996**.
- [27] R. J. Flook, C. H. Freeman, C. J. Moore, M. L. Scudder, *Chem. Commun.* **1973**, 753.
- [28] C. I. H. Ashby, W. F. Paton, T. L. Brown, *J. Am. Chem. Soc.* **1980**, *102*, 2990.
- [29] T. Takayama, S. Ohuchida, Y. Koike, M. Watanabe, D. Hashizume, Y. Ohashi, *Bull. Chem. Soc. Jpn.* **1996**, *69*, 1579.
- [30] H. Maumela, R. D. Hancock, L. Carlton, J. H. Reibenspies, K. P. Wainwright, *J. Am. Chem. Soc.* **1995**, *117*, 6698.
- [31] E. Kimura, T. Koike, T. Shiota, Y. Iitaka, *Inorg. Chem.* **1990**, *29*, 4621.
- [32] H. Thiel, U. Weber, A. Germanus, K. Il'yasov, *WIN-Dynamics*, Bruker-Franzen-Analytik, Bremen (Germany), **1995**.
- [33] C. Cox, H. Wack, T. Lectka, *J. Am. Chem. Soc.* **1999**, *121*, 7963.
- [34] D. L. Rabenstein, T. Shi, S. Spain, *J. Am. Chem. Soc.* **2000**, *122*, 2401.
- [35] L. M. Sayre, K. V. Reddy, A. R. Jacobson, W. Tang, *Inorg. Chem.* **1992**, *31*, 935.
- [36] L. M. Berreau, M. M. Makowska-Grzyska, A. M. Arif, *Inorg. Chem.* **2000**, *39*, 4390.
- [37] C. Meplan, K. Mann, P. Hainaut, *J. Biol. Chem.* **1999**, *274*, 31 663.
- [38] G. W. Buchko, N. J. Hess, M. A. Kennedy, *Carcinogenesis* **2000**, *21*, 1051.
- [39] J. Stöckel, J. Safar, A. C. Wallace, F. E. Cohen, S. B. Prusiner, *Biochemistry* **1998**, *37*, 7185.
- [40] A. I. Bush, *Curr. Op. Chem. Biol.* **2000**, *4*, 184.
- [41] L. M. Sayre, G. Perry, C. S. Atwood, M. A. Smith, *Cell. Mol. Biol.* **2000**, *46*, 731.
- [42] B. S. Wong, T. Pan, T. Liu, R. L. Li, R. B. Petersen, I. M. Jones, P. Gambetti, D. R. Brown, M. S. Sy, *Biochem. Biophys. Res. Commun.* **2000**, *275*, 249.
- [43] J. H. Viles, F. E. Cohen, S. B. Prusiner, D. B. Goodin, P. Wright, H. J. Dyson, *Proc. Natl. Acad. Sci. USA* **1999**, *96*, 2042.
- [44] T. Miura, A. Hori-i, H. Mototani, H. Takeuchi, *Biochemistry* **1999**, *38*, 11 560.
- [45] R. P. Bonomo, G. Impellizzeri, G. Pappalardo, E. Rizzarelli, G. Tabbi, *Chem. Eur. J.* **2000**, *6*, 4195.
- [46] E. Aronoff-Spencer, C. S. Burns, N. I. Avdievich, G. J. Gerfen, J. Peisach, W. E. Antholine, H. L. Ball, F. E. Cohen, S. B. Prusiner, G. L. Millhauser, *Biochemistry* **2000**, *39*, 13 760.
- [47] J. K. Romary, R. D. Zachariasen, J. D. Barger, H. Schiesser, *J. Chem. Soc. Dalton Trans. C* **1968**, 2884.
- [48] F. Hojland, H. Toftlund, S. Yde-Andersen, *Acta Chem. Scand.* **1983**, *A 37*, 251.
- [49] a) A. C. T. North, D. C. Phillips, F. S. Mathews, *Acta Cryst. A* **1968**, *351*; b) "Collect" data collection software, Nonius B.V., Delft **1998**; c) "Scalepack" data processing software, Z. Otwinowski, W. Minor, *Methods Enzymol.* **1997**, *276*, 307.
- [50] A. Altomare, G. Casciarano, C. Giacovazzo, A. Guagliardi, *J. Appl. Cryst.* **1993**, *26*, 343.
- [51] G. M. Sheldrick, *SHELXTL-PC* Siemens Analytical X-ray Instruments Inc., Madison, WI (USA), **1994**.
- [52] G. M. Sheldrick, *SHELXL-97*, Universität Göttingen, **1997**.
- [53] H. Günther, *NMR-Spektroskopie*, 2nd ed., Georg Thieme, Stuttgart/New York, **1983**.

Received: January 5, 2001
Revised July 20, 2001 [F2986]